Australian Journal of Crop Science AJCS

AJCS 17(11):816-821 (2023) ISSN:1835-2707
doi: 10.21475/ajcs.23.17.11.p3866

Assessment of orbital sensors in estimating sugarcane crop evapotranspiration with the “*SAFER*” algorithm

Carlos Cesar Silva Jardim, José Alves Júnior*, Derblai Casaroli, Adão Wagner Pêgo Evangelista, Rafael Battisti

School of Agronomy, Department of Soil and Water, Federal University of Goias (UFG), Zip code 74.690.900, Goiania, Goias, Brazil

***Corresponding author: josealvesufg@ufg.br**

Abstract

Understanding sugarcane water demand is important for planting planning, yield estimation, irrigation management, forecasting and water resources management. The purpose of this study was to estimate the evapotranspiration of the variety RB985476 in 2nd. re-grow, from August/2017 to September/2018, in a mechanized harvest area and with straw distribution over dystrophic red Latosolo, through the SAFER algorithm, with two passive orbital image sensors: Landsat 8 and Sentinel 2. The results demonstrated that SAFER better estimated ETc from Landsat 8 images and that remote sensing is not efficient for ETc estimation in phenological stages with low plant coverage. The sensors show divergences in surface and albedo temperature estimates and no difference in NDVI estimation was observed. The landsat 8 products are superior in evapotranspiration estimates when compared to the standards recommended in this paper.

Keywords: Saccharum spp.; water demand; water requirement; remote sensing
Abbreviations: ETc_culture evapotranspiration, Alb_24 albedo in 24 hours; LST_surface temperature; NDVI_vegetation index of the normalized red band difference.

Introduction

The cultivation of sugarcane in Brazil has been an important commercial activity since the colonial period, and is still one of the most cultivated crops in the whole territory. The regions with the highest production are concentrated in the Southeast and Center-West (85% of the area and total production), for the production of alcohol, sugar, and cogeneration of electric energy (Souza et al., 2018).

In addition to the current prominence of the Brazilian Midwest, this region presents a growing panorama of sugarcane expansion. However, the expansion of sugarcane in this region is limited by a significant water deficit compared to the traditional sugarcane producing regions in the Southwest, and by the limited number of sugarcane varieties adapted to this condition (Nocelli et al., 2017).

In this way, research agencies work on management strategies to minimize the impact caused by regional differences in varieties imported from other regions (Reis et al., 2014).

In the absence of information, the crops are grown in order to ensure that the period of highest water deficit does not coincide with the stage of highest crop water demand (Ribeiro et al., 2015). In addition, knowing the water requirement, given the maximum crop evapotranspiration at each stage of its development, is also important in the use of simulation models of productivity, and irrigation management, both for full irrigation and for supplementary irrigation (Collicchio et al., 2015), besides being fundamental in the calculation of irrigation project outflows and water resources management.

Evapotranspiration can be measured in situ using direct methods for example lysimeters or evapotranspirometers, and using indirect methods for calculating water balance in the soil and energy balance, but in both cases, the accuracy of these methodologies should be measured by region and culture (Miranda et al., 2016; Paiva and Souza, 2016). Between the methods of energy balance, remote sensing has been widely used to obtain the evapotranspiration of several crops (Sales et al., 2016; 2018; Dias et al., 2019; Oliveira et al., 2019; Sales et al., 2018).

For remote sensing evapotranspiration estimation, images can be obtained by free orbital imaging sensors (satellites), including: Landsat 8, Sentinel 2 and MODIS (Petropoulos, 2013; Thenkabail, 2016); and algorithms are more common: SEBAL (Surface Energy Balance Algorithm for Land) (Bastiaanssen et al., 1998), METRIC (Mapping EvapoTranspiration at High Resolution using Internalized Calibration) (Allen et al., 2007) and SAFER (Simple Algorithm for Evapotranspiration Retrieving) (Teixeira, 2010).

There are significant differences in estimates between imaging sensors based on the development characteristics of the satellites, being these different in spatial, spectral and radiometric resolution, and these differences affect the observation of the Earth's surface (Bezerra et al., 2018; Pardo-Pascual et al., 2018).

For the characterization of the surface, there are standardization techniques so that independently of the sensors present different characteristics, they can represent the object. However, corrections are not always sufficient for

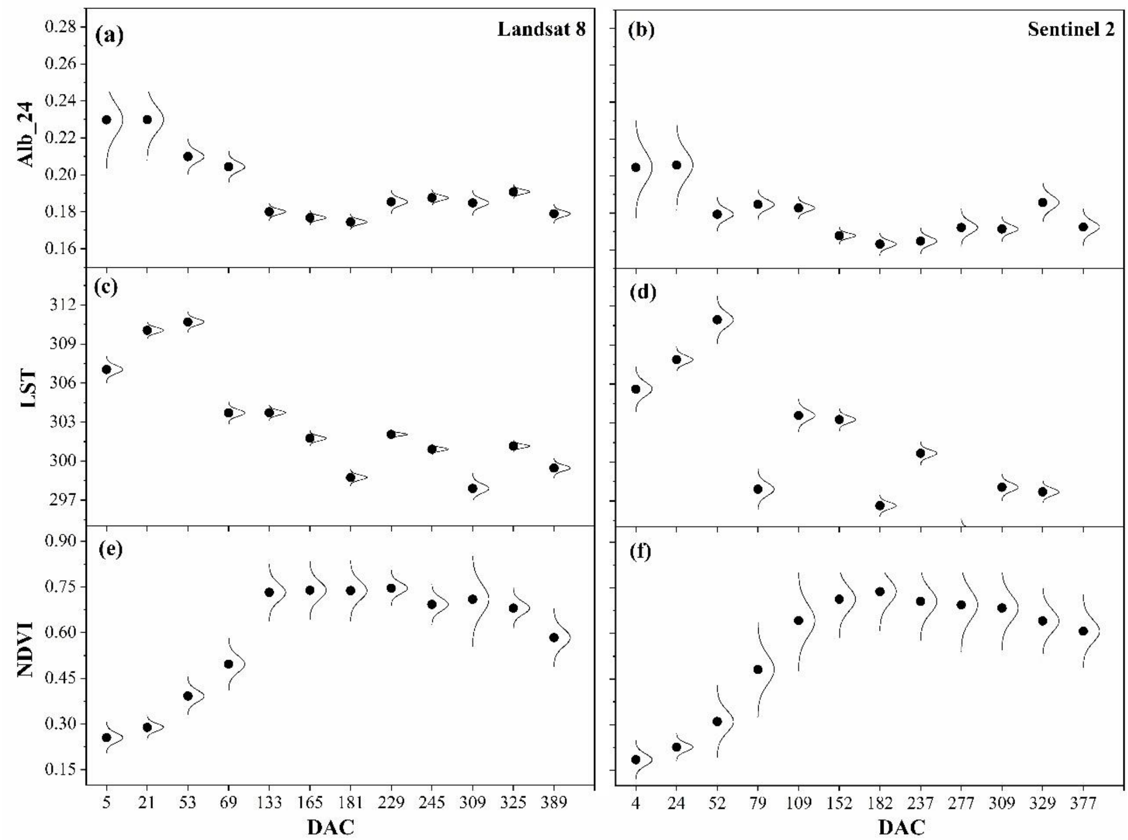

Figure 1. Seasonal variation of parameters used in the SAFER algorithm during the sugarcane cycle, for albedo in 24 hours (Alb_24) for Landsat 8 (a) and Sentinel 2 (b), surface temperature (LST, °K) for Landsat 8 (c) and Sentinel 2 (d) and vegetation index of the normalized red band difference (NDVI) for Landsat 8 (e) and Sentinel 2 (f).

this, because besides presenting radiometric and spectral differences, the source of error may come from the spatial difference in image between the sensors. For some characteristics of the surface, the sensors present similar estimates, since the variation is not significant, but already for the detection of shades within the same phytophysiology, satellites with larger spatial resolutions present more details and allow the differentiation of objects through indexes or highlights of reflectance (Amaral, 2009; Thenkabail, 2016).

Thus, the objective of this study was to verify the temporal variation in the estimate of evapotranspiration of sugarcane culture in Mato Grosso do Sul, through the SAFER algorithm, with two passive orbital imaging sensors.

Results and Discussion

Satellite sensor products

The satellite images (Landsat 8 and Sentinel 2) demonstrated that the more vegetation the plants have grown, the smaller the reflectance values, as well as the higher the vegetation indexes (NDVI) values were observed. For surface albedo, sugarcane presented an average of 18.5% of total light reflectance (Figures 1 a, b), concentrating in the canopy a large part of the intercepted energy. For the beginning of the cycle, plants in the beginning of re-growth with straw covered soil, this value was higher (22%). Similar results were found by Oliveira et al. (2015) and Moraes and Oliveira (2019), who found a variation of 13 to 20% of the surface albedo, in the phases of full development and initial phase respectively, using MODIS Sensor (250x250 m).

For the temperature of vegetated surface, no oscillations were observed in the normal distribution for Landsat 8, due to the spatial resolution being smaller than Sentinel 2, which in turn presents higher oscillation, demonstrated both by the temporal variation of the means and the amplitude of the distribution by date (Figure 1 c, d). The Sentinel 2 has a pixel of 10x10 m differing characteristics such as terraces, and tipping spots, while the Landsat 8, with a resolution of 30x30 m does not identify these patterns.

The temperature values of the vegetated sugarcane surface may indicate if there is physiological stress due to water deficit (Trentin et al., 2011), where the comparison between the increase in leaf temperature at the expense of air temperature demonstrates moments of stress for the plant. And for higher surface temperature values also correspond to the time of low leaf area, contribution of straw and/or exposed soil (Ramos, 2017).

The NDVI demonstrated the evolutionary behavior of the crop, where from 100 days on, the crop showed total coverage of the area, and maximum vegetative growth (Figures 1 E and 1 F). The averages for the two sensors are 0.75, and for Sentinel 2, the variation was greater due to the detection of the irregularity in the vegetated surface. Other studies show that the use of images allows the modeling of morphological aspects of the culture, demonstrating the evolution of the leaf area (Pereira et al., 2016), while allowing the correlation of NDVI with the physiological and nutritional state of the culture (Alface et al., 2019)

Statistical agrometeorological components

The comparison of ETr/ETo results obtained via SAFER algorithm, showed that in initial periods (90 days of regrowth), with low expressivity of plants, it does not present significant results (Figure 2). For the Landsat 8 satellite, the

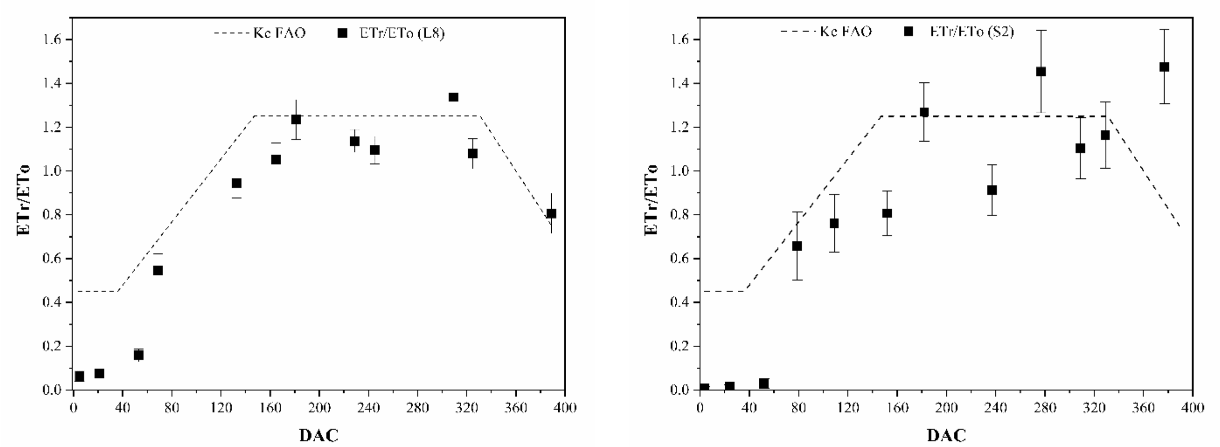

Figure 2. Comparison of the ETr/ET0 versus the culture coefficient (Kc) proposed by FAO 56.

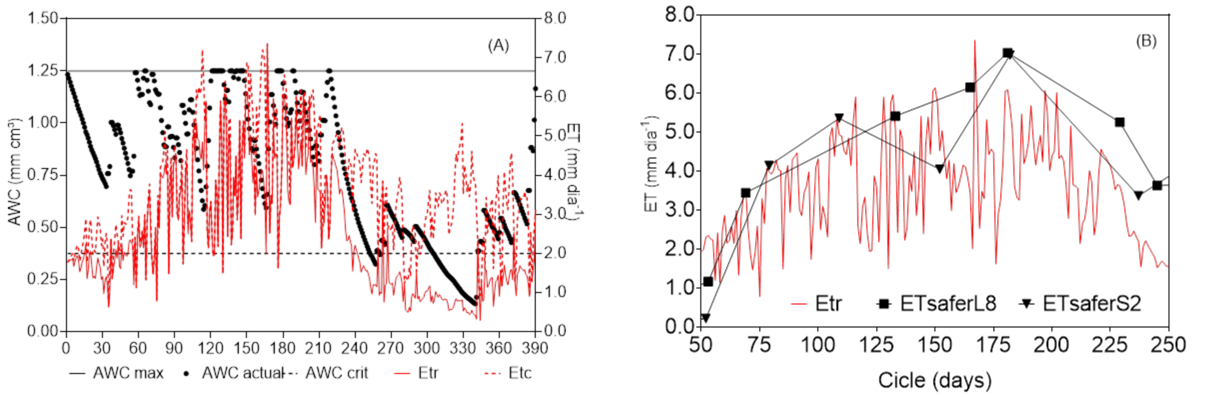

Figure 3. (A) - Crop Evapotranspiration (ETc), Actual Evapotranspiration (ETr), Maximum Water Soil Storage Capacity (AWC max), Critical Water Soil Storage Capacity (AWC crit) and Current Water Soil Storage Capacity (AWC actual). (B) - Actual crop evapotranspiration, current Landsat 8 Evapotranspiration and current Sentinel 2 Evapotranspiration in period without water restriction.

Table 1. Statistical indexes for adjustment of values estimated by the SAFER algorithm using the Sentinel 2 and Landsat 8 satellite in comparison to those expected by FAO 56 for the period without water restriction.

	d	R	c
	Sentinel 2		
ETr/ETo	0.64	0.67	0.43
ETr	0.75	0.71	0.53
	Landsat 8		
ETr/ETo	0.90	0.96	0.86
ETr	0.87	0.94	0.82

Coefficient "c": >0.85 Good; 0.76 to 0.85 Very good; 0.66 to 0.75 Good; 0.61 to 0.65 Fair; 0.51 to 0.60 Acceptable; 0.41 to 0.50 Bad; ≤ 0.40 Terrible.

ETr/ETo averages were close to the maximum expected in periods without water restriction, being inferior due to the area being dry, and the precipitation not being uniform during the cycle. For Sentinel 2 the estimates were affected by the surface temperature variation, making the estimates oscillate both in the imaging date and temporally.

The calibration of parameters "a" and "b" of the algorithm is fundamental for local estimation, as it affects the inclination of the response surface of the NDVI variables, surface temperature and albedo in the estimation of ETr/ETo. Estimates with parameters 1 and -0.008 ("a" and "b") respectively, point to a maximum ETr/ETo of 0.55, a value much lower than the expected for the crop, therefore, an underestimate (Feitosa et al., 2016), while 1.8 and -0.008 the values are close to the expected maximum and in some cases inferring a higher coefficient for phases of higher demand (Silva et al., 2019).

The estimation of actual crop evapotranspiration by the two satellites presents moments of adjustment with the actual evapotranspiration by the method of water balance in the soil, and for the period of 60 to 220 days of re-growth (DAC) there was significant rainfall for the maintenance of soil moisture (Figure 3). For Landsat 8 the variation occurs in lower intensity than for Sentinel 2, which in turn presents underestimations in most of the cycle, and abrupt variations with overestimations at different times.

The algorithm presented an adjustment for the evapotranspiration estimation for both rainy and dry periods, as long as the plant is established (Teixeira et al., 2016). While the impact of the estimation of the variable "surface temperature" has a relation to the pixel size, causing disuniformity of the estimates when considered long cycle

and passive bedding cultures, or due to radiometric difference of the imaging sensors (Silva et al., 2019).
The calculated statistical indices demonstrate the temporal dispersion of ETr/ETo and ETr estimates compared to the FAO standard of culture coefficient and potential evapotranspiration by Penman-Monteith (Table 1). The adjustment coefficients for Landsat 8 are higher than Sentinel 2, and for Wilmott dispersion is 26% and 12% (ETr/ETo and ETr) more accurate, for Pearson correlation is very strong for Landsat 8 and moderate to strong for Sentinel 2, Landsat 8 has over 29% and 23% (ETr/ETo and ETr) more precision than Sentinel 2, and the concordance rate for Landsat 8 classified as very good and great, and for Sentinel 2 as bad to acceptable.
The superiority of the Landsat 8 adjustment can be due to the radiometric differences of the sensors, and the presence of thermal band in its constitution, while Sentinel 2 uses temperature estimation by the residual method of the image. Adjustments of the coefficients "a" and "b" of the algorithm considering the local characteristics, and the study material can increase the accuracy of the estimates.

Materials and methods

Conduction of study and experimental design
The study was carried out in an 11 hectare commercial sugarcane field, in second cut cultivation, with the variety RB985476, at 1.5 m spacing between lines, with subsequent harvest of the cana-plant. A mechanized harvester with a spreading device of straw was used, located in the municipality of Jutí-MS (22° 51' 18.0" S; 54° 40' 00.6" O). According to Köppen, the climate in the region is of the Cfa type, a sub-tropical climate with hot temperatures in summer, and average annual precipitation of 1500 mm. It shows a change in temperatures due to altitude and transition zones between geographical formations, with the possibility of frost in the colder months (Alvares et al., 2013). The soil of the region is predominantly Red Latosol Distrófico (93%), containing small areas with presence of Quartz Neosols (5%).

Orbital and agrometrological series data
The data collection of the orbital sensors was carried out from August/2017 to September/2018, finishing with the harvest of the first cycle of crop regrowth in September 2018.
The meteorological data were obtained from NASA/POWER database. From these, it was realized the hydric balance of the culture, using the methodology proposed by Thornthwhaite and Mather (Pereira, 2005). Reference evapotranspiration (ETo) was obtained using the Penman-Monteith-FAO method (Allen et al., 1998). According to Negm et al. (2018), the data obtained via remote sensing are assertive for modeling the energy flux and gas exchange in agriculture, using different models for obtaining evapotranspiration.
The multispectral images of the area were acquired at the USGS Explorer/NASA portal, where only scenes without cloud interference in the region were selected, thus reducing the possibility of shading. For the Sentinel 2 satellite images, the images already have atmospheric reflectance corrections, and for the use of algorithms were redesigned for the WGS 84 datum, in geographic coordinates, and the files formed the base date for the generation of evapotranspiration products, reflectance, energy flow and vegetation elements. For the base date of the Landsat 8 satellite the transformation of the available images was performed, and for temporal data comparison the conversion of DN (digital number) into absolute reflectance was performed, called Reflectance at the top of the atmosphere (TOA) of the observed scene, where the equation provided by the USGS explorer (Eq. [1]) was used:

$$\rho\lambda' = M\rho * Qcal + A\rho \quad [1]$$

Where: ρλ' is the reflectance at the top of the atmosphere without correction of the solar angle, Mρ the multiplicative scaling factor of the reflectance for the band used, Qcal the digital number of the pixel in the band used, Aρ the additive scaling factor of reflectance for the band used.
The values for equation 1, were found in the metadata that make up the package provided by the catalog and, due to the location of the study area is inclined to the path of the sun for much of the period, with the balance of variable solar radiation, the correction of solar slope was made on the dates of evaluation (Eq.[2]):

$$\rho\lambda = \frac{\rho\lambda\prime}{sen(\theta)} \quad [2]$$

Where: ρλ: reflectance at the top of the atmosphere corrected, ρλ': reflectance at the top of the atmosphere without correction of the solar angle, θ: solar elevation angle.
After the treatment of the images, it was proceeded the determination of the reflective characteristics of the culture, where for this were calculated the albedo of the surface in the top of the atmosphere, vegetation index by normalized difference in the red band (NDVI), balance of radiation and temperature of the surface, being thus possible the implementation of the algorithm SAFER (Simple Algorithm for Evapotranspiration Retrieving), which made possible the determination of the instantaneous evapotranspiration of the culture (Eq.[3]):

$$\frac{ET}{ET0} = \exp\left[a + b\left(\frac{T_0}{\alpha_0 * NDVI}\right)\right] \quad [3]$$

Where: In what: ET: instantaneous evapotranspiration (mm), ETo: reference evapotranspiration (mm), a and b;: adjustment coefficients (1.8 and -0.008, respectively) proposed by (TEIXEIRA et al., 2016), T0: surface temperature (°K), ∝0: surface albedo at the top of the atmosphere, NDVI: vegetation index by normalized difference in the red band.
In addition, reference evapotranspiration values, obtained on the imaging date, calculated by the Penman- Monteith-FAO equation (Allen et al., 1998), are inserted to obtain instantaneous evapotranspiration (Eq.[4]):

$$ETc = \frac{ET}{ETo} * ETo \quad [4]$$

Where: ETc: crop evapotranspiration (mm)
In assessing the estimated data, they were compared by the maximum expected value in the observation phases for the crop according to FAO bulletin 56, being determined the evapotranspirations of sugarcane crop through equation (Eq.[5]):

$$ETc = ET0 * kc \quad [5]$$

Where: kc: coefficient of culture 0.45 for initial phases (35 days); 1.25 for full development (±295 days); 0.75 for maturation phase (±60 days))
The data obtained were evaluated as to dispersion by means of exploratory analysis with descriptive statistics for the determination of the estimated properties for sugarcane, being: correlation coefficient "r" of Pearson (Eq.[6]), index of concordance "d" of Willmott et al. (1985) (Eq.[7]), and confidence coefficient "c" (Sentelhas et al., 1997) (Eq.[8]):

$$r = \frac{\Sigma(xi-\bar{x})(yi-\bar{y})}{\sqrt{[\Sigma((xi-\bar{x})^2] \, [\Sigma(yi-\bar{y})^2]}} \quad [6]$$

$$d = 1 - \frac{\Sigma yi-xi^2}{\Sigma(|yi-\bar{x}|+|xi-\bar{x}|)^2} \quad [7]$$

$c = r \cdot d$ [8]

Where: Xi: observed evapotranspiration, ⍰:average of observed evapotranspiration, Yi: estimated evapotranspiration, and ⍰: average of observed evapotranspiration.

Conclusions

The SAFER algorithm in general presents correlation, adjustment and superior reliability for the Landsat 8 satellite in relation to the Sentinel 2, in the estimation of sugarcane evapotranspiration, when compared with that established by FAO for periods without water restriction. Periods of low plant coverage do not offer adjustment of the estimates of evapotranspiration, requiring greater attention in this period. The sensors present divergences for the estimation of the algorithm input variables, being in higher order of difference for surface temperature, lower for albedo inferring different evapotranspirations. There is no significant difference in NDVI. Factors such as surfaces coverage and water restriction may interfere with the quality of evapotranspiration measurement through orbital sensors and the SAFER algorithm.

Acknowledgments

The authors acknowledge Coordination of Improvement of Higher Education Personnel (CAPES) and National Council for Scientific and Technological Development (CNPq) for the research and productivity support provided to the authors, and Interuniversity Network for the Development of the Sugar and Energy Sector (RIDESA) for the research funding in the development of algorithms for the evaluation of this paper.

References

Amaral MVF, Souza AL de, Soares VP, Soares CPB, Leite HG, Martins SV, Fernandes Filho EI and Lana JM de (2009) Avaliação e compação de métodos de classificação de imagens de satélites para o mapeamento de estádios de sucessão florestal. Rev Árvore. 33: 575–582.

Alface AB, Pereira SB, Filgueiras R and Cunha FF, (2019) Sugarcane spatial-temporal monitoring and crop coefficient estimation through NDVI. Rev Bras Eng Agríc Ambient. 23: 330–335.

Allen RG, Pereira LS, Raes D, Smith M (1998) Crop Evapotranspiration: Guidelines for Computing Crop Water Requirements – FAO Irrigation and Drainage Paper 56. Food and Agriculture Organization of the United Nations: Rome, Italy, 300p.

Allen, RG, Tasumi, M and Trezza, R, (2007) Satellite-Based Energy Balance for Mapping Evapotranspiration with Internalized Calibration (METRIC)-Model. Journal of Irrigation and Drainage Engineering. 133: 380–394.

Bastiaanssen WGM, Menenti M, Feddes RA, Holtslag AAM (1998) A remote sensing surface energy balance algorithm for land (SEBAL): 1. Formulation. Journal of Hydrology. 212/213:198-212.

Bezerra UA, Oliveira LMM, Candeias ALB, Silva BB, Leite ACLS and Silva LTMS, (2018) Comparison of the Normalized Difference Vegetation Index (NDVI) Between the Sensors OLI-Landsat Satellite-8 and MSI-Sentinel-2 Satellite in Semi-Arid Region. Anuário IGEO UFRJ. 41: 167–177.

Collicchio E, Rocha HRD, Victoria D de C, Ballester MVR and Toledo AMA (2015) Implicações das mudanças do clima no zoneamento agroclimático da cana-de-açúcar no estado do Tocantins, considerando o modelo GFDL. Revista Brasileira de Geografia Física, Recife. 8(6):1730-1747.

Dias TL, Porto Rodrigues A, Raik Arcanjo Batista M, Vicente MR and Medeiros Dos Santos R (2019) Evapotranspiração e coeficiente de cultura do cafeeiro irrigado a partir de imagens de sensores orbitais. R_I. 1: 31–37.

Feitosa DG, Hernandez FB, Franco RAM, Teixeira AHC and Neale CM (2016) Energy balance in the watershed of Ipê, Northwestern São Paulo State, Brazil, in: Neale, C.M.U., Maltese, A. (Eds.), . Presented at the SPIE Remote Sensing, Edinburgh, United Kingdom, p. 99980O.

Miranda WL, Carvalho LG, Castro Neto P and Santos PAB (2016) Utilização do lisímetro de drenagem para obtenção do "Kc" da mamoneira em plantio adensado. Revista Verde. 11: 08.

Moraes EC and Oliveira BS (2019) Avaliação da acurácia do albedo do modis para a cultura de cana-de- açucar no nordeste. In: SIMPÓSIO BRASILEIRO DE SENSORIAMENTO REMOTO.

Nocelli R, Zambon V, Silva O and Morini M (2017) Histórico da cana-de-açúcar no Brasil: contribuições e importância econômica. pp. 13–30.

Oliveira BS, Moraes EC, Rudorff BFT, Mataveli GAV (2015) Análise do desempenho de modelos de albedo da superfície em áreas de cana-de-açúcar com dados do sensor modis/terra. Revista Brasileira de Cartografia. v. 67.

Oliveira DA, Hernandez FBT, Bispo RC, Teixeira AHC (2019) Aplicação do algoritmo safer para determinação da evapotranspiração em canaviais irrigados por diferentes sistemas. IRRIGA. 1(1): 1–7.

Paiva CM, Souza, ASP (2016) Evaluation of Methods for Reference Evapotranspiration Estimation for Irrigation Water Management. Anuário do Instituto de Geociências - UFRJ, 39(1): p. 42.

Pardo-Pascual J, Sánchez-García E, Almonacid-Caballer J, Palomar-Vázquez J, Priego SE, Fernández-Sarría A, Balaguer-Beser Á (2018) Assessing the accuracy of automatically extracted shorelines on microtidal beaches from Landsat 7, Landsat 8 and Sentinel-2 Imagery. Remote Sensing. 10(2): 326.

Pereira RM, Casaroli D, Vellame LM, Alves Júnior J, Evangelista AWP (2016) Estimativa da área foliar de cana-de-açúcar a partir do índice de vegetação por diferença normalizada (NDVI) corrigido. Pesquisa Agropecuária Tropical (Agricultural Research in the Tropics).p. 140–148.

Petropoulos GP (2013) Remote Sensing of Energy Fluxes and Soil Moisture Content. CRC Press.

Ramos RRD (2017) Evapotranspiração da cana-de-açúcar utilizando o simple algorithm for evapotranspiration retrieving (safer) no Vale São Francisco. p. 5, In: congresso brasileiro de agrometeorologia, simpósio de mudanças climáticas e desertificação no semiárido brasileiro, Juazeiro, BA. A agrometeorologia na solução de problemas multiescala: anais. Petrolina: Embrapa Semiárido; Juazeiro: UNIVASF; Campinas: Sociedade Brasileira de Agrometeorologia.

Reis RR, Andrade DCB, Martins PK, Martins MTB, Alekcevetch JC, Chalfun-Júnior A, Andrade AC, Ribeiro AP, Qin F, Mizoi J, Yamaguchi-Shinozaki K, Nakashima K, Carvalho JFC, Sousa CAF, Nepomuceno AL, Kobayashi AK, Molinari, HBC (2014) Induced over-expression of AtDREB2A CA improves drought tolerance in sugarcane. Plant Science. 221–222:59–68.

Ribeiro RC, Dallacort R, Barbieri JD (2015) Zoneamento do saldo hídrico anual da cana-de-açúcar para o estado de mato grosso. ENCICLOPÉDIA BIOSFERA, p. 13.

Sales DLA, Alves Júnior J, Souza JMF, Casaroli D, Evangelista, AWP, Pereira, RM (2016) Common bean evapotranspiration estimated by orbital images. African Journal of Agricultural Research. 11, 867-872.

Sales DLA, Alves Júnior J, Casaroli D, Evangelista AWP, Souza JMF (2018) Estimativa de evapotranspiração e coeficiente de cultura do tomateiro industrial utilizando o algoritmo safer. IRRIGA. 22(3): 629–640.

Silva COF, Manzione RL, Albuquerque Filho JL (2019) Modelagem da evapotranspiração com imagens sentinel-2 e landsat-8. In: Anais do XIX simpósio brasileiro de sensoriamento remoto, Santos. Anais eletrônicos.. Campinas, GALOÁ.

Souza G, Gurgel A, Feres JG (2018) Sugarcane expansion scenarios and their impacts on land use and food production in Brazil: exercises based on a computable general equilibrium model. International Association of Agricultural Economists. 2018 Conference, July 28-August 2, 2018, Vancouver, British Columbia 277303.

Teixeira AHC (2010) Determining regional actual evapotranspiration of irrigated and natural vegetation in the São Francisco river basin (Brazil) using remote sensing an Penman-Monteith equation. Remote Sensing. 1287-1319.

Teixeira AHC, Leivas JF, Ronquim CC, Bayma-Silva G, Victoria DC (2016) Energy balances in sugar cane, coffee and natural vegetation in the northeastern side of the São Paulo state, Brazil. In: Remote sensing for agriculture, ecosystems, and hydrology XVIII 2016, Anais... . In: Remote sensing for agriculture, ecosystems, and Hydrology XVIII. : International Society for Optics and Photonics.

Thenkabail PS (2016) Remote sensing of water resources, disasters, and urban studies. Boca Raton: Taylor & Francis.

Trentin R, Zolnier S, Ribeiro A, Steidle Neto AJ (2011) Transpiração e temperatura foliar da cana-de-açúcar sob diferentes valores de potencial matricial. Engenharia Agrícola, 31(6), p. 1085–1095.